ACS APPLIED MATERIALS & INTERFACES

Research Article

www.acsami.org

# Endocytic Mechanisms of Graphene Oxide Nanosheets in Osteoblasts, Hepatocytes and Macrophages

Javier Linares,[†] M. Concepción Matesanz,[†] Mercedes Vila,[‡,§,⊥] M. José Feito,[†] Gil Gonçalves,[⊥] María Vallet-Regí,[‡,§] Paula A. A. P. Marques,[⊥] and M. Teresa Portolés*[,†]

[†]Department of Biochemistry and Molecular Biology I, Faculty of Chemistry, Universidad Complutense, 28040 Madrid, Spain

[‡]Department of Inorganic and Bioinorganic Chemistry, Faculty of Pharmacy, Instituto de Investigación Sanitaria Hospital 12 de Octubre i+12, Universidad Complutense, 28040 Madrid, Spain

[§]Networking Research Center on Bioengineering, Biomaterials and Nanomedicine, CIBER-BBN, 50018 Aragon, Spain

[⊥]TEMA-NRD, Mechanical Engineering Department, University of Aveiro, 3810-193 Aveiro, Portugal

**ABSTRACT:** Nano-graphene oxide (GO) has attracted great interest in nanomedicine due to its own intrinsic properties and its possible biomedical applications such as drug delivery, tissue engineering and hyperthermia cancer therapy. However, the toxicity of GO nanosheets is not yet well-known and it is necessary to understand its entry mechanisms into mammalian cells in order to avoid cell damage and human toxicity. In the present study, the cellular uptake of pegylated GO nanosheets of ca. 100 nm labeled with fluorescein isothiocyanate (FITC-PEG-GOs) has been evaluated in the presence of eight inhibitors (colchicine, wortmannin, amiloride, cytochalasin B, cytochalasin D, genistein, phenylarsine oxide and chlorpromazine) that specifically affect different endocytosis mechanisms. Three cell types were chosen for this study: human Saos-2 osteoblasts, human HepG2 hepatocytes and murine RAW-264.7 macrophages. The results show that different mechanisms take part in FITC-PEG-GOs uptake, depending on the characteristics of each cell type. However, macropinocytosis seems to be a general internalization process in the three cell lines analyzed. Besides macropinocytosis, FITC-PEG-GOs can enter through pathways dependent on microtubules in Saos-2 osteoblasts, and through clathrin-dependent mechanisms in HepG2 hepatocytes and RAW-264.7 macrophages. HepG2 cells can also phagocytize FITC-PEG-GOs. These findings help to understand the interactions at the interface of GO nanosheets and mammalian cells and must be considered in further studies focused on their use for biomedical applications.

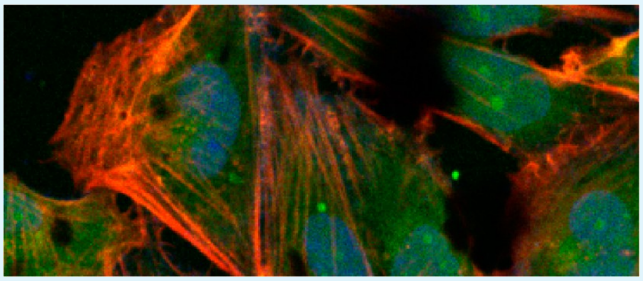

**KEYWORDS:** *endocytosis, graphene oxide, hepatocyte, macrophage, nanoparticle, osteoblast*

## INTRODUCTION

Nano-graphene oxide (GO) and its functionalized derivatives have attracted great interest in nanomedicine due to its own intrinsic properties, all the dimensions lower than 100 nm and a singular chemical structure,[1] which allows interesting possible biomedical applications such as drug delivery,[2,3] tissue engineering[4,5] and hyperthermia cancer therapy.[6−8] The evaluation of the interactions at the interface of GO nanosheets and mammalian cells must be carried out before this nanomaterial can be used for biomedical applications. Concerning GO administration, although GO colloids are soluble in water, they need further functionalization with molecules like poly(ethylene glycol-amine) (PEG), which improves the material dispersion and stability in aqueous solutions.[2,9] Previous studies with PEGylated GO nanosheets labeled with fluorescein isothiocyanate (FITC-PEG-GOs) revealed differences in the amount of FITC-PEG-GOs uptake by Saos-2 osteoblasts, L929 fibroblasts, RAW-264.7 macrophages and MC3T3-E1 preosteoblasts as a function of the cell type involved. Thus, FITC-PEG-GOs uptake was higher and faster in osteoblasts than in the other three cell types without inducing cell membrane damage.[10] Recent studies evidenced that for doses of 75 $\mu$g/mL, after cell internalization, FITC-PEG-GOs are preferentially localized on F-actin filaments, inducing cell-cycle alterations, apoptosis and oxidative stress in these cell types.[11] Concerning the potential use of nano-graphene oxide for hyperthermia cancer therapy, preliminary studies have shown effective induction of cell death in vitro after irradiating tumoral osteoblasts with internalized PEG-GOs.[6] However, the study of the toxicology of these nanosheets is still in its very early stages and it is necessary to know the entry mechanisms of PEG-GOs into mammalian cells for assessing its human toxicity. External nanoparticles can interact with the plasma membrane and enter into cells through different endocytosis processes. Two main types of endocytosis are distinguished depending on the size of the endocytic

Received: May 21, 2014
Accepted: June 30, 2014
Published: June 30, 2014

  

vesicles formed due to the particle size: phagocytosis (particles larger than 0.5 μm) and pinocytosis (uptake of fluids and solutes).[12] Phagocytosis is characteristic of specialized phagocytes such as macrophages, neutrophils, monocytes and dendritic cells. Nanoparticles that enter into cells through phagocytosis are recognized by different opsonins such as immunoglobulins, complement components and serum proteins. Then the opsonized nanoparticles bind to the cell surface, inducing the cup-shaped membrane extension to form the phagosomes, which move into cells to fuse with lysosomes. Pinocytosis is carried out in all cell types and presents multiple forms depending on the cell type and function. The most recent classification of pinocytosis is based on the proteins involved in the different pathways of this endocytic process. Thus, pinocytosis is classified in "clathrin-mediated endocytosis" and "clathrin-independent endocytosis".[13] The clathrin-independent pathways are further classified as (a) caveolae-mediated endocytosis, (b) clathrin- and caveolae-independent endocytosis and (c) macropinocytosis. Clathrin- and caveolae-independent pathways are subclassified as Arf6-dependent, flotillin-dependent, Cdc42-dependent and RhoA-dependent endocytosis.[14] Recent studies with protein-coated graphene oxide nanosheets indicate that small nanosheets enter cells mainly through clathrin-mediated endocytosis, and the increase of graphene size enhances its phagocytotic uptake by C2C12 cells.[15]

In the present study, the cellular uptake of pegylated GO nanosheets labeled with fluorescein isothiocyanate (FITC-PEG-GOs) has been evaluated in the presence of several inhibitors that specifically affect different endocytosis mechanisms. Three cell types have been chosen taking into account their origin and specific reasons: (a) human Saos-2 osteoblasts, because the FITC-PEG-GOs uptake by these osteoblast-like cells was higher and faster than by other cell types without resulting in cell membrane damage;[10,11] (b) human HepG2 hepatocytes, because when a nanomaterial is placed in contact with the human body, proteins adsorb to its surface, activating cellular and molecular mechanisms, which leads to fast elimination by the liver;[16,17] (c) murine RAW-264.7 macrophages, because after in vivo administration, the triggering of immunological processes leads to a reduction of the circulation half-life of nanoparticles in the bloodstream by macrophages, which culminates in a reduction of biodistribution and often the impossibility of achieving the specific targets.[8]

## EXPERIMENTAL SECTION

**Preparation and Characterization of GO Nanosheets.** GO nanosheets have been prepared following the method previously published by the authors.[10] Basically, GO nanosheets of ca. 100 nm (GOs) were obtained from exfoliation of high purity graphite in acidic medium by a modified Hummers method.[18] The resulting GOs suspension was then dialyzed until a pH of 7, activated to promote −COOH groups at its surface and functionalized by covalent bonding with nontoxic and nonimmunogenic polymer poly(ethylene glycol-amine) (1-arm PEG, 1.5 kDa) to avoid the intercession with cellular functions or target immunogenicities and to decrease aggregation.[10] The sample was marked with the amine reactive dye fluorescein isothiocyanate (FITC) covalently bonded to the PEG. Transmission electron microscopy (TEM) was performed on a 200 kV JEOL JEM 2100. FITC-PEG-GOs were analyzed by atomic force microscopy (AFM, VEECO multimode, USA.) and Fourier transform infrared spectroscopy (FTIR, Nicolet Nexus spectrometer). Dynamic light scattering (DLS) particle size analysis measurements were also performed in pH 5 solutions in a Zetasizer Nano series instrument equipped with a 633 nm "red" laser from Malvern Instruments with reproducibility being verified by collection and comparison of sequential measurements. Z-average sizes of three sequential measurements were collected at room temperature (RT) and analyzed.

For checking the successful fluorescence labeling after PEGylation, the amino content of the 1-arm-PEG-GO was determined at every synthesis step by quantitative analysis of the amino groups in order to monitor the chemical modifications.

**Cell Culture for Incorporation of FITC-PEG-GOs and Previous Treatment with Endocytosis Inhibitors.** Saos-2 osteoblasts, HepG2 hepatocytes and RAW-264.7 macrophages were seeded on 6-well culture plates (CULTEK) at a density of $10^5$ cells/mL in Dulbecco's modified Eagle's medium (DMEM) supplemented with 10% fetal bovine serum (FBS, Gibco), 1 mM L-glutamine (BioWhittaker), penicillin (200 μg/mL, BioWhittaker) and streptomycin (200 μg/mL, BioWhittaker), under a 5% $CO_2$ atmosphere and at 37 °C. After 48 h, different endocytosis inhibitors were added separately to the culture medium and the cells were maintained for 2 h under a 5% $CO_2$ atmosphere and at 37 °C. The inhibitors used in these assays were 2.5 μM colchicine (Alexis-Enzo), 23 μM wortmannin (Biomol-Enzo), 1 mM amiloride (Alexis-Enzo), 20 μM cytochalasin B (MP Biomedicals), 4 μM cytochalasin D (MP Biomedicals), 37 μM genistein (Alexis-Enzo), 3.7 μM phenylarsine oxide (PAO, Sigma-Aldrich) and 30 μM chlorpromazine (Alexis-Enzo). The dose of each inhibitor was chosen taking into account the previous studies carried out by different research groups.[18−26] After 2 h of treatment with these inhibitors, the culture medium was removed and fresh medium with 37.5 μg/mL FITC-PEG-GOs was added to the cultures, which were maintained for 2 h under a 5% $CO_2$ atmosphere and at 37 °C. Then, cells were harvested using either 0.25% trypsin−EDTA (in Saos-2 and HepG2 cells) or cell scrapers (in RAW-264.7 cells) and counted with a Neubauer hemocytometer. For evaluating the FITC-PEG-GOs incorporation, the fluorescence of FITC was excited at 488 nm and measured with a 530/30 band-pass filter in a FACScalibur Becton Dickinson flow cytometer. Two control types were carried out in parallel: (a) Control, which corresponds to cells without inhibitors and without FITC-PEG-GOs and (b) Control + GO, which corresponds to cells without inhibitors but with FITC-PEG-GOs.

**Cell Viability Measurements.** After culture with FITC-PEG-GOs in the presence or the absence of different endocytosis inhibitors, cells were detached and incubated with propidium iodide (PI; 0.005% in PBS, Sigma-Aldrich) to stain the DNA of dead cells. The PI exclusion indicates the plasma membrane integrity and cell viability. The fluorescence of PI was excited at 488 nm and the emission was measured with a 670 nm LP in a FACScalibur Becton Dickinson flow cytometer.

**Confocal Microscopy Studies.** Cells were seeded on glass coverslips and cultured with FITC-PEG-GOs for 2 h in the presence or the absence of different endocytosis inhibitors, fixed with 3.7% paraformaldehyde in PBS, permeabilizated with 0.1% Triton X-100 and preincubated with PBS containing 1% BSA. Then, cells were incubated for 20 min with rhodamine phalloidin (1:40), stained with 4′-6-diamidino-2′-phenylindole (DAPI, 3 μM in PBS) and examined using a Leica SP2 confocal laser scanning microscope. Rhodamine fluorescence was excited at 540 nm and measured at 565 nm. DAPI fluorescence was excited at 405 nm and measured at 420−480 nm. FITC fluorescence was excited at 488 nm and measured at 491−586 nm.

**Inflammatory Cytokine Detection.** IL-6 cytokine released by cells to the culture medium was quantified by ELISA with a Gen-Probe Diaclone kit.

**Statistics.** Data are expressed as means ± standard deviations of a representative of three experiments carried out in triplicate. Statistical analysis was performed using the Statistical Package for the Social Sciences (SPSS) version 19 software. Statistical comparisons were made by analysis of variance (ANOVA). A Scheffé test was used for post hoc evaluations of differences among groups. In all of the statistical evaluations, $p < 0.05$ was considered as statistically significant.

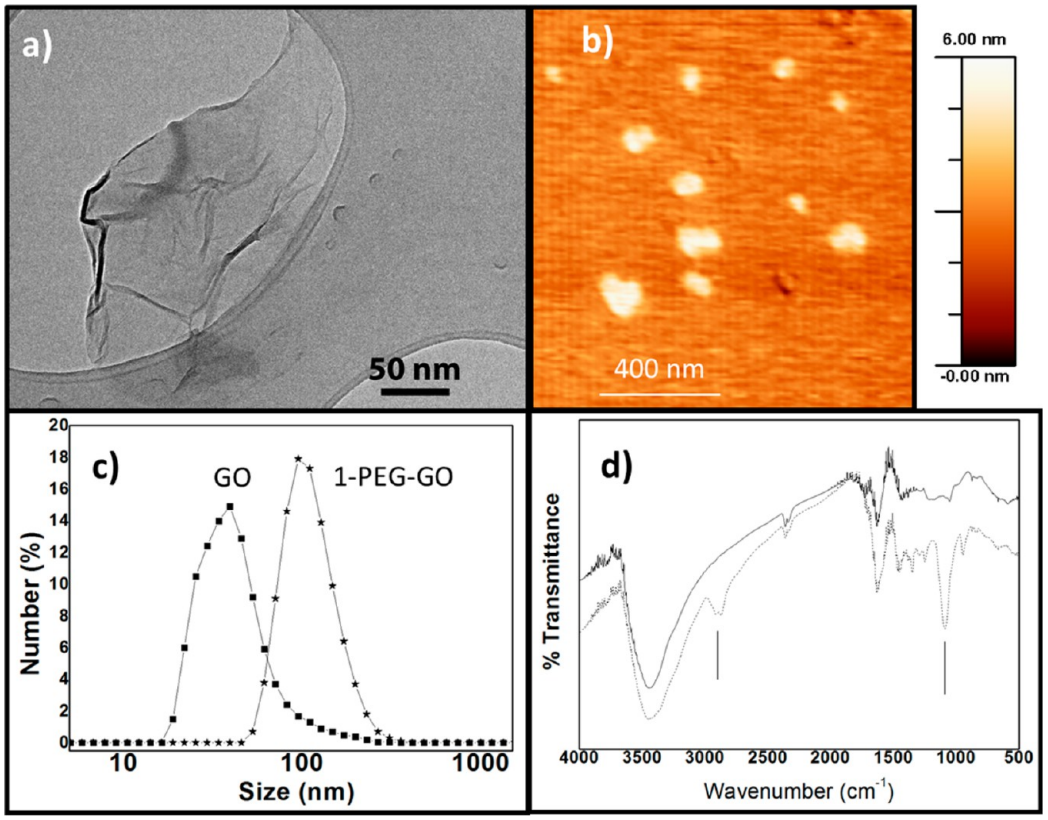


**Figure 1.** (a) Transmission electron micrograph of GO nanosheets. (b) AFM topographic image of dispersed GO nanosheets. (c) GO nanosheets particle size distribution obtained by DLS. (d) FTIR spectra of GO nanosheets and PEGylated GO nanosheets.

## RESULTS AND DISCUSSION

The study of the interaction of nanomaterials with cells and their entry mechanisms is necessary as a previous step for their application in biomedicine. These interactions are not only affected by surface and size factors but also strongly depend on cell types.[8,10,11,27,28] The aim of the present study was to know the mechanisms of endocytosis involved in the internalization of GO nanosheets (GOs) of ca. 100 nm, functionalized with PEG and marked with FITC (FITC-PEG-GOs), into Saos-2 osteoblasts, HepG2 hepatocytes and RAW-264.7 macrophages.

Graphene oxide (GO) has been of great interest in applications like biomaterials. However, its large lateral dimensions avoid the cellular internalization. In that sense, the potential of that material resides in the decrease of size to a nanometric scale at all the dimensions (nano-GO). After submitting GO to ultrasounds in an acidic medium, it is possible to obtain a sharp decrease in particle size, as can be observed on TEM and AFM images in Figure 1a,b. As it can be observed, GO nanosheets are formed by flexible sheets with 2 or 3 layers of graphene. Dynamic light scattering (DLS) analysis confirmed the imaging techniques by giving a final GO average size of 80 nm prior to PEGylation (Figure 1c). Once the PEG polymer is covalently bonded, the hydrodynamic size increases up to an average size of 100 nm.

The functionalization of GO with PEG chains is an important step that avoids opsonization and consequently removal of nanoparticles from the bloodstream by macrophages, decreasing its lifetime on the body. FTIR analysis clearly indicates the presence of the PEG chains at the surface of GO platforms by adding to the presence of the oxygen functionalities at GO surface, the C−O stretch vibration band (1100−1150 $cm^{-1}$) and the strong C−H stretch peak (2800 $cm^{-1}$).

Values of the amine quantification for having a direct measure of the average quantity of amines before and after fluorescent labeling on 1-arm pegylated GOs are shown in Table 1, showing a decrease in the amino content after FITC linking synthesis, directly implying a successful FITC linking.

**Table 1. Quantitative Analysis of Amine Content ($10^{-5}$ mmol $mg^{-1}$)**

| GO | GO-PEG | GO-PEG-FITC |
|---|---|---|
| 1.3 | 1.52 | 1.47 |

The functionalization of GOs by covalently bonding with 1-arm PEG has been carried out because it decreases aggregation, avoids the intercession with cellular functions or target immunogenicities and also reduces protein adsorption and nonspecific uptake by macrophages, which allows these GOs to have a long blood circulation half-life.[10] These PEG-GO nanosheets have previously shown effective internalization and induction of cell death in vitro after irradiating tumoral osteoblasts.[6]

Figure 2 shows the values of FITC-PEG-GOs incorporation by cultured Saos-2, HepG2 and RAW-264.7 cells and its effects on viability and cell number after 2 h of treatment in the absence of inhibitors. Significant incorporation differences were observed among these cell types, obtaining higher values in osteoblasts and hepatocytes than in macrophages, in agreement with the demonstrated higher uptake of smaller particles by cells in which phagocytosis is not the main endocytosis

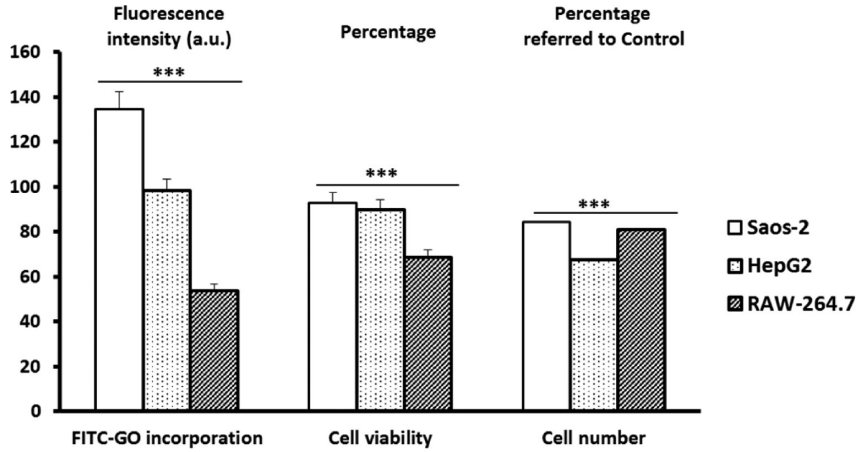


**Figure 2.** FITC-PEG-GOs incorporation by cultured Saos-2, HepG2 and RAW-264.7 cells and its effects on cell viability and cell number after 2 h of treatment in the absence of inhibitors. ***, $p < 0.005$ (compared to Control without FITC-PEG-GOs).

**Scheme 1. Steps for Indirect Measurement of FITC-PEG-GOs Endocytic Mechanisms with Specific Endocytosis Inhibitors**

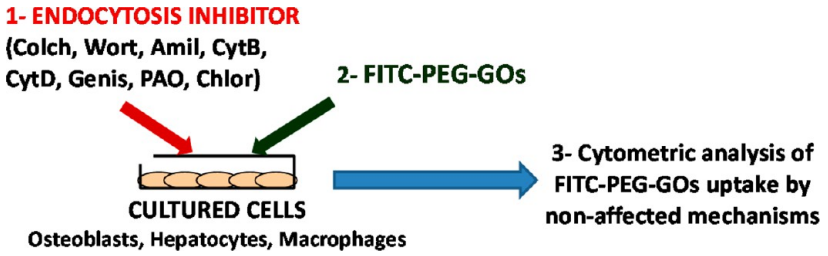


**Table 2. Effects of Specific Endocytosis Inhibitors Indicating the Affected Mechanism, the Altered Protein Target and the References Concerning the Action of each Compound**

| endocytosis inhibitors | | | |
|---|---|---|---|
| inhibitor | affected mechanism | target | references |
| colchicine | mitosis | tubulin: microtubule polymerization alteration and cell cycle arrest in metaphase. | 19 |
| wortmannin | phagocytosis | PI3K (selective) and other kinases as miosine light chain kinase and PI4K. | 20 |
| amiloride | macropinocytosis | $Na^+/H^+$ exchanger. Unspecific. | 21 |
| cytochalasin B | macropinocytosis | actin: blockage of its polymerization avoiding microfilaments action. | 22 |
| cytochalasin D | macropinocytosis | actin: blockage of its polymerization avoiding microfilaments action and inhibition of other endocytosis routes. | 23 |
| genistein | clathrin-independent endocytosis | caveolae: inhibition of Src tyrosine kinases and caveolae dynamics. | 24 |
| phenylarsine oxide (PAO) | clathrin-dependent endocytosis | tyrosine phosphatases: membrane fluidity decrease and thiol groups oxidation. | 22, 25, 26 |
| chlorpromazine | clathrin-dependent endocytosis | clathrin: alteration of clathrin-coat assembly, membrane fluidity and permeability. | 23 |

mechanism.[11] On the other hand, the properties of PEG, used to functionalize GOs in the present study, limit the interaction with biological interfaces and also decrease the particle uptake by macrophages, increasing their circulation time as indicated above.[9,10] Although the highest uptake was obtained in Saos-2 cells and the lowest incorporation in RAW-264.7 cells, RAW viability was more affected by the FITC-PEG-GOs treatment than this parameter in osteoblasts and hepatocytes, which showed values over 80−90% after treatment. A slight but significant decrease in the cell number produced by contact with this material was also observed in all cases, in comparison with the controls without FITC-PEG-GOs, as reported previously for this dose.[10,11] The higher effect of FITC-PEG-GOs on HepG2 proliferation than on Saos-2 and RAW-264.7 proliferation can be due to the characteristics of HepG2 cells, which are slower growing cells that have a high tendency for cell−cell attachment.

It must be taken into account that the FITC-PEG-GOs dose used in the present study was chosen because previous assays with this dose have shown good results concerning incorporation and cell viability[10,11] as well as an effective induction of cell death in vitro after irradiating tumoral osteoblasts with internalized PEG-GO nanosheets.[6] The evaluation of the plasma membrane integrity is one of the most common ways to measure cell viability and cytotoxic effects. This parameter, analyzed through propidium iodide exclusion in the present study and through lactate dehydrogenase release in previous assays,[10] reveals high viability levels and indicates that the FITC-PEG-GOs dose used in our studies does not induce plasma membrane damage. However, previous studies have shown that the FITC-PEG-GOs uptake produces

significant increases of reactive oxygen species (ROS) in MC3T3-E1 preosteoblasts and RAW-264.7 macrophages but not in Saos-2 osteoblasts.[11]

To understand the endocytic mechanisms involved in FITC-PEG-GOs uptake by cultured Saos-2 osteoblasts, HepG2 hepatocytes and RAW-264.7 macrophages, eight specific endocytosis inhibitors (colchicine, wortmannin, amiloride, cytochalasin B, cytochalasin D, genistein, phenylarsine oxide and chlorpromazine) were added to the culture medium before FITC-PEG-GOs treatment to know the effects of each agent on the material entry into each cell type. Scheme 1 shows the steps carried out in the present study for the indirect measurement of FITC-PEG-GOs endocytic mechanisms after treatment of cultured osteoblasts, hepatocytes and macrophages with specific endocytosis inhibitors and flow cytometric analysis.

Table 2 shows the mechanism affected by each inhibitor, the protein target that is altered after its binding and the references concerning the action of these compounds. The dose of each inhibitor used in these experiments was chosen according to the references in Table 2. Figure 3 shows the effects of each inhibitor on FITC-PEG-GOs incorporation by Saos-2, HepG2 and RAW-264.7 cells. Cultures were treated for 2 h with each inhibitor, then the medium was removed and fresh medium with 37.5 $\mu$g/mL FITC-PEG-GOs was added and maintained for 2 h. The results evidence the coexistence of different mechanisms for FITC-PEG-GOs uptake, and their dependence on the characteristics of each cell type.

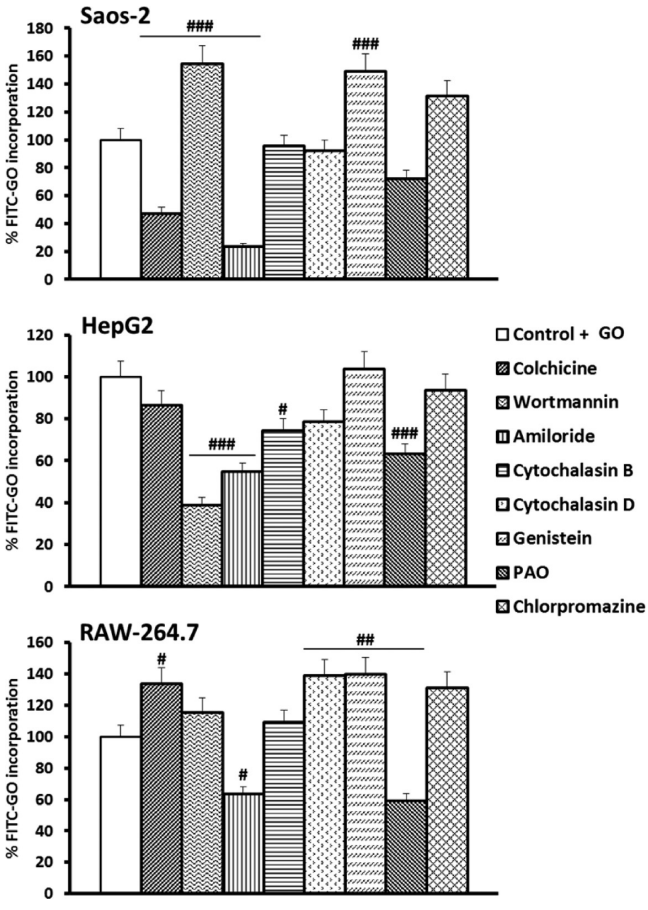


**Figure 3.** Effects of specific endocytosis inhibitors on FITC-PEG-GOs incorporation by cultured Saos-2, HepG2 and RAW-264.7 cells. Cultures were treated for 2 h with each inhibitor, then the medium was removed and fresh medium with 37.5 $\mu$g/mL FITC-PEG-GOs was added and maintained for 2 h. Controls without inhibitors but with FITC-PEG-GOs (Control + GO) were carried out in parallel. #, $p < 0.05$; ##, $p < 0.01$; ###, $p < 0.005$ (compared to Control + GO).

Concerning Saos-2 osteoblasts, colchicine and amiloride produce a significant FITC-PEG-GOs incorporation decrease, suggesting the entry through pathways dependent on microtubules (affected by colchicine) and macropinocytosis mechanisms (affected by amiloride). Macropinocytosis comprises a series of events initiated by extensive plasma membrane reorganization or ruffling to form an external macropinocytic structure that is then enclosed and internalized. Macropinosomes share many features with phagosomes and both are distinguished from other forms of pinocytic vesicles by their large size, morphological heterogeneity and lack of coat structures.[29] Macropinocytosis is dependent on microtubule function because these elements are involved in plasma membrane ruffling and also are necessary for transport of GTPases that mediate macropinocytosis to specific plasma membrane domains where they can be activated.[30] The pronounced effect of amiloride, which inhibits macropinocytosis by lowering submembranous pH and preventing Rac1 and Cdc42 signaling,[31] demonstrates that this endocytosis mechanism is the main process for FITC-PEG-GOs entry into Saos-2 cells. However, the doses used of cytochalasins B and D, which inhibit macropinocytosis by actin polymerization blockage avoiding microfilaments action,[23,24] did not reduce the FITC-PEG-GOs incorporation by this cell type at these experimental conditions.

As it can be observed in Figure 3, the treatments with either wortmannin or genistein significantly increase FITC-PEG-GOs uptake by Saos-2 osteoblasts. Wortmannin inhibits phosphoinositide 3-kinase (PI3K) and phosphoinositide 4-kinase (PI4K),[20] which play important roles in many cellular processes such as cell motility, adhesion, proliferation, apoptosis and cytoskeletal organization,[32] affecting phagocytosis mechanisms. Genistein produces inhibition of Src tyrosine kinases and caveolae dynamics.[24] Because wortmannin and genistein did not decrease FITC-PEG-GOs incorporation by osteoblasts, phagocytosis and caveolae-mediated uptake are not mechanisms involved in the FITC-PEG-GOs uptake by this cell type at these experimental conditions. On the other hand, the action of these inhibitors seems to increase the entry of this material through other mechanisms that are not blocked for these treatments. The doses of phenylarsine oxide (PAO) and chlorpromazine used in this study did not induce statistically significant effects on Saos-2 cells, thus suggesting that clathrin-dependent endocytosis is not involved in the GO incorporation by this cell type.

Concerning FITC-PEG-GOs incorporation by HepG2 hepatocytes, significant decreases were observed after treatment with wortmannin, amiloride, cytochalasin B and phenylarsine oxide (PAO). Because both macropinocytosis inhibitors, amiloride,[21] and cytochalasin B,[22] significantly decreased FITC-PEG-GOs uptake by hepatocytes, the results indicate again that macropinocytosis is the main mechanism for FITC-PEG-GOs entry into this cell type too. Colchicine and cytochalasin D also produced slight diminutions with the doses used in the present study, but these effects were not statistically significant after data analysis.

The inhibition produced by wortmannin, specific inhibitor of phagocytosis,[20] evidence that hepatocytes can phagocytize FITC-PEG-GOs in agreement with the capability of this cell

type described by other authors to uptake silicon particles and exogenous substances.[33] Polarized hepatic cells present endocytosis via phosphoinositide 3-kinase of resident apical plasma membrane proteins.[34] The significant decrease of FITC-PEG-GOs entry produced by PAO (inhibitor of clathrin-dependent endocytosis)[22,25,26] and the absence of genistein effect (inhibitor of clathrin-independent endocytosis mediated by caveolae),[24] indicate the role of clathrin-dependent endocytic pathway in FITC-PEG-GOs uptake by hepatocytes. HepG2 cells have no endogenous caveolin, so they are unable to uptake nanoparticles by caveolae-mediated endocytosis.[35] Chlorpromazine, inhibitor of clathrin-dependent mechanisms,[23] also produced a slight diminution of FITC-PEG-GOs incorporation by HepG2 cells but it was not statistically significant at these experimental conditions. Thus, macropinocytosis, phagocytosis and clathrin-dependent endocytic pathways can be involved in the fast elimination of GO nanosheets by the liver.[16,17]

Concerning FITC-PEG-GOs incorporation by RAW-264.7 macrophages, amiloride and PAO treatments produced significant FITC-PEG-GOs entry decreases, thus indicating the existence of macropinocytosis[21] and clathrin-dependent mechanisms,[22,25,26] respectively, for the internalization of this nanomaterial into RAW cells. However, cytochalasin B and chlorpromazine, which also are inhibitors of macropinocytosis[22] and clathrin-dependent mechanisms,[23] respectively, did not produce an effect on FITC-PEG-GOs uptake by this cell type with the doses and assay conditions used. In this sense, the dose of wortmannin used in the present study according to other references[20] was not enough to inhibit the active phagocytosis carried out by RAW macrophages, which has been observed in previous studies with these cells and other materials.[33] Colchicine (microtubule polymerization alteration),[19] cytochalasin D (actin polimerization blockage)[23] and genistein (inhibition of caveolae dynamics)[24] seem to increase the entry of FITC-PEG-GOs through other mechanisms probably due to cytoskeletal alterations which makes this structure more accessible for FITC-PEG-GOs binding, in agreement with previous studies, which indicates the specific localization of FITC-PEG-GOs on F-actin filaments of different cell types.[11]

Figure 4 shows the effects of these specific endocytosis inhibitors and FITC-PEG-GOs on cell viability of cultured Saos-2, HepG2 and RAW-264.7 cells in comparison with controls carried out in parallel without inhibitors and without materials. Although high viability values were obtained with Saos-2 osteoblasts after these treatments, amiloride and PAO inhibitors induced a significant and pronounced decrease of this parameter, indicating the toxicity of both compounds.

Cytochalasin B produced a slight significant viability decrease in Saos-2 cells, although high viability values were obtained in the presence of this inhibitor (80%). However, in HepG2 hepatocytes, only amiloride produced a significant viability decrease to 70%, demonstrating the higher resistance of this cell type to all these inhibitors and to GO. Although RAW-264.7 cells showed more sensitivity to all these treatments, specially to PAO, amiloride did not induce significant changes in the viability of these macrophages.

It must be taken into account that the dose of each inhibitor was chosen after considering the previous studies carried out by different research groups.[18−26] Although some inhibitors produced cell damage in the experimental conditions of the present study, the results evidence that several processes are

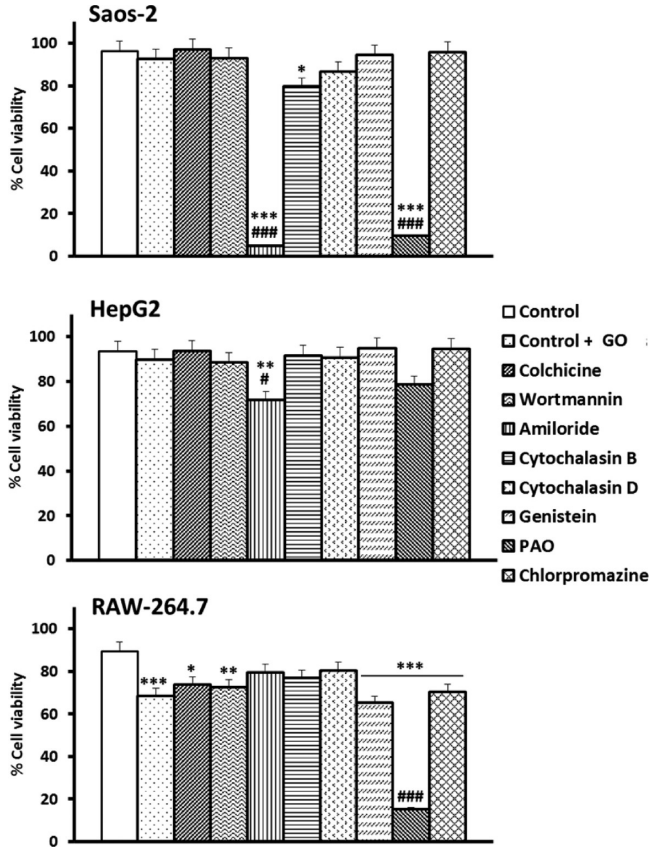


**Figure 4.** Effects of specific endocytosis inhibitors and FITC-PEG-GOs on cell viability of cultured Saos-2, HepG2 and RAW-264.7 cells. Cultures were treated for 2 h with each inhibitor, then the medium was removed and fresh medium with 37.5 $\mu$g/mL FITC-PEG-GOs was added and maintained for 2 h. *, $p < 0.05$; **, $p < 0.01$; ***$p$, $< 0.005$ (compared to Control carried out without inhibitors and without material). #, $p < 0.05$; ###$p < 0.005$ (compared to Control + GO carried out without inhibitors but with FITC-PEG-GOs).

involved in FITC-PEG-GOs uptake, depending on the characteristics of each cell type.

On the other hand, because in previous studies FITC-PEG-GOs induced in Saos-2 osteoblasts a significant decrease of IL-6 levels at longer times (72 h),[11] the production of these proinflammatory cytokine was evaluated in the culture medium after treatment of Saos-2 cells with each specific endocytosis inhibitor and in the two situations: before or after FITC-PEG-GOs addition. Figure 5 shows the values of IL-6 levels in each situation compared with controls carried out in parallel without treatment (horizontal line). As it can be observed, no significant differences on this cytokine were obtained before and after 2 h of FITC-PEG-GOs addition to cells without inhibitor treatment (Control + GO in the figure). However, significant IL-6 increases were observed in the culture medium of Saos-2 cells that were previously treated with endocytosis inhibitors except in the cases of wortmannin and amiloride, which were more pronounced after FITC-PEG-GOs addition in almost all cases. The treatment with these two inhibitors did not produce significant IL-6 changes before FITC-PEG-GOs addition but wortmannin decreased significantly the IL-6 levels after FITC-PEG-GOs addition and amiloride increased significantly this parameter after FITC-PEG-GOs addition to cells.

These data must be taken into account in further studies focused on the effects of GOs incorporation on cellular

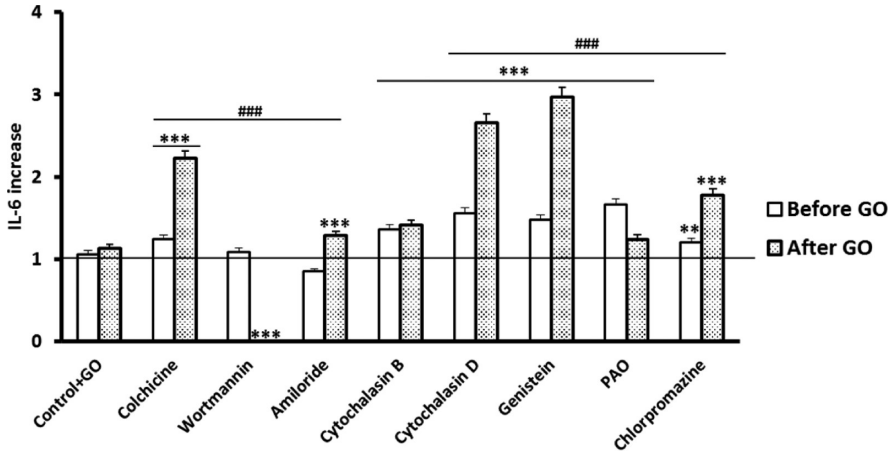


**Figure 5.** Effects of specific endocytosis inhibitors and FITC-PEG-GOs on the production of IL-6 evaluated in the culture medium after treatment of Saos-2 cells with each inhibitor and before or after FITC-PEG-GOs treatment. The values were compared with controls carried out in parallel without treatment. **, $p < 0.01$; ***, $p < 0.005$ (compared to control without treatment, horizontal line). ###, $p < 0.005$ (comparing before and after FITC-PEG-GOs addition).

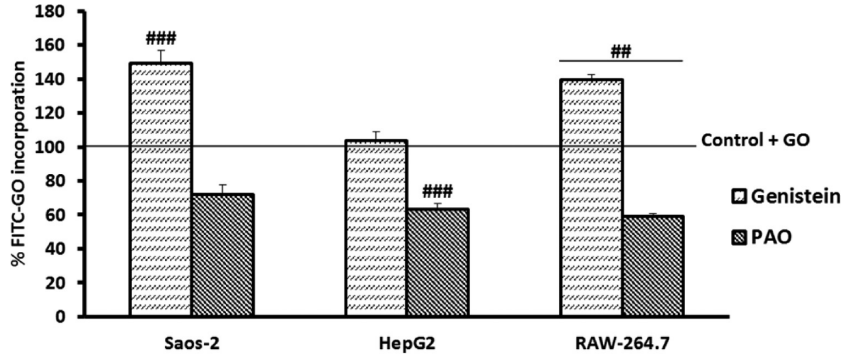


**Figure 6.** Effects of genistein and PAO on FITC-PEG-GOs incorporation by cultured Saos-2, HepG2 and RAW-264.7 cells. Cultures were treated for 2 h with each inhibitor, then the medium was removed and fresh medium with 37.5 $\mu$g/mL FITC-PEG-GOs was added and maintained for 2 h. The percentages are referred to controls with FITC-PEG-GOs but without inhibitors carried out in parallel (Control + GO, horizontal line). ##, $p < 0.01$; ###, $p < 0.005$.

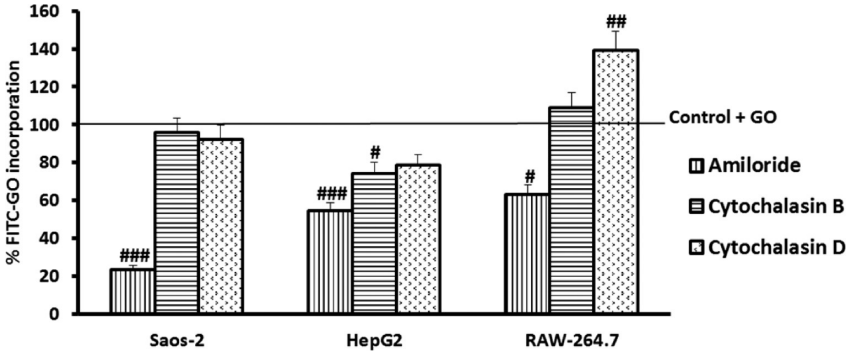


**Figure 7.** Effects of amiloride, cytochalasin B and cytochalasin D on FITC-PEG-GOs incorporation by cultured Saos-2, HepG2 and RAW-264.7 cells. Cultures were treated for 2 h with each inhibitor, then the medium was removed and fresh medium with 37.5 $\mu$g/mL FITC-PEG-GOs was added and maintained for 2 h. The percentages are referred to controls with FITC-PEG-GOs but without inhibitors carried out in parallel (Control + GO, horizontal line). #, $p < 0.05$; ##, $p < 0.01$; ###, $p < 0.005$.

functions in the presence of these agents. On the other hand, the action of wortmannin, which inhibits phosphoinositide 3-kinase (PI3K) and phosphoinositide 4-kinase (PI4K),[20] is in agreement with the effects of this inhibitor on IL-6 production observed with osteoarthritis synovial fibroblasts.[36]

In Figure 6 are summarized the effects of genistein and PAO on FITC-PEG-GOs incorporation by cultured Saos-2, HepG2 and RAW-264.7 cells. Values are expressed as percentages referred to cultures treated with FITC-PEG-GOs but without inhibitors carried out in parallel. The figure demonstrates the opposite action of genistein (which acts inhibiting Src tyrosine kinases and caveolae dynamics)[24] and PAO (which inhibits tyrosine phosphatases, producing membrane fludity decreases).[22,25,26] These two inhibitors affect clathrin-independ-

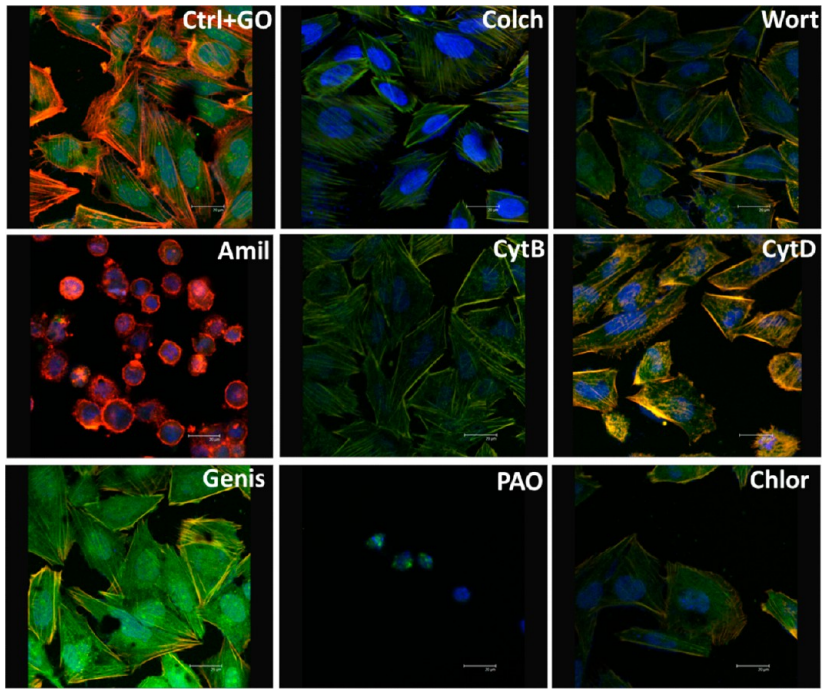


**Figure 8.** Morphology evaluation by confocal microscopy of cultured human Saos-2 osteoblasts after treatment with specific endocytosis inhibitors and FITC-PEG-GOs. Cells were stained with DAPI for the visualization of the cell nuclei in blue, rhodamine phalloidin for the visualization of cytoplasmic F-actin filaments in red and FITC for the visualization of FITC-PEG-GOs in green. Ctrl+GO = control with FITC-PEG-GOs and without inhibitors, Colch = colchicine, Wort = wortmannin, Amil = amiloride, CytB = cytochalasin B, CytD = cytochalasin D, Genis = genistein, PAO = phenylarsine oxide and Chlor = chlorpromazine.

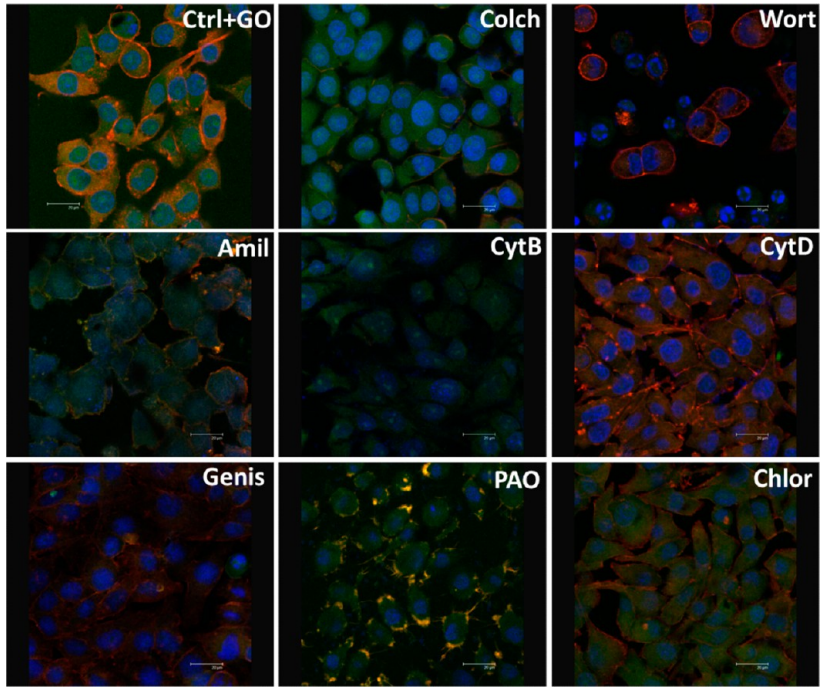


**Figure 9.** Morphology evaluation by confocal microscopy of cultured human HepG2 hepatocytes after treatment with specific endocytosis inhibitors and FITC-PEG-GOs. Cells were stained with DAPI for the visualization of the cell nuclei in blue, rhodamine phalloidin for the visualization of cytoplasmic F-actin filaments in red and FITC for the visualization of FITC-PEG-GOs in green. Ctrl+GO = control with FITC-PEG-GOs and without inhibitors, Colch = colchicine, Wort = wortmannin, Amil = amiloride, CytB = cytochalasin B, CytD = cytochalasin D, Genis = genistein, PAO = phenylarsine oxide and Chlor = chlorpromazine.

ent and clathrin-dependent endocytosis, respectively, through these kind of enzymes, tyrosine kinases and tyrosine phosphatases, with opposite effects.

In Figure 7 are summarized the effects of amiloride, cytochalasin B and cytochalasin D on FITC-PEG-GOs incorporation by cultured Saos-2, HepG2 and RAW-264.7

cells. Values are expressed as percentages referred to cultures treated with FITC-PEG-GOs but without inhibitors carried out in parallel. The pronounced effect of amiloride, which inhibits macropinocytosis by lowering submembranous pH and preventing Rac1 and Cdc42 signaling,[31] demonstrates that this endocytosis mechanism is the main process for FITC-PEG-GOs entry into osteoblasts, hepatocytes and macrophages. However, the doses used of cytochalasins B and D, which inhibit macropinocytosis by actin polymerization blockage avoiding microfilaments action,[23,24] only were effective on HepG2 cells at these experimental conditions.

Because Saos-2 and HepG2 cells showed higher FITC-PEG-GOs incorporation than RAW macrophages, confocal microscopy studies were carried out with these two cell types to evaluate their morphology after treatment with these eight endocytosis inhibitors and FITC-PEG-GOs. Figures 8 and 9 correspond to confocal images of osteoblasts and hepatocytes, respectively, showing FITC-PEG-GOs (in green), rhodamine phalloidin (to stain F-actin filaments in red) and DAPI (for nuclear staining in blue) after each inhibitor treatment.

The evaluation of human Saos-2 osteoblast morphology after treatment with specific endocytosis inhibitors and FITC-PEG-GOs (Figure 8) evidence the typical characteristics of this cell type with cube-shaped morphology except after treatment with amiloride and PAO, in agreement with the effect of these inhibitors on cell viability (Figure 4). Osteoblasts control with FITC-PEG-GOs and, without inhibitors, show colocalization of FITC-PEG-GOs (green) and F-actin (red), in agreement with previous results.[11] The lowest FITC-PEG-GOs incorporation is observed after amiloride treatment, as results in Figure 3 also confirm. The highest FITC-PEG-GOs incorporation by osteoblasts observed by confocal microscopy corresponds to the samples treated with genistein, in agreement with the flow cytometric analysis (Figure 3). Because green fluorescence is not decreased with genistein, it confirms that caveolae-mediated uptake is not involved in the FITC-PEG-GOs incorporation by this cell type. This inhibitor seems to increase the entry of FITC-PEG-GOs through other mechanisms, which could be related to enhanced plasma membrane fluidity.[24] Confocal images of Saos-2 osteoblasts treated with amiloride allow us to suggest the FITC-PEG-GOs incorporation through pathways dependent on macropinocytosis mechanisms.[21]

Figure 9 shows the morphology evaluation by confocal microscopy of cultured human HepG2 hepatocytes after treatment with specific endocytosis inhibitors and FITC-PEG-GOs. After all these treatments, this cell type maintains its polygonal characteristic shape, in agreement with the viability values obtained (Figure 4). Hepatocytes control with FITC-PEG-GOs and without inhibitors also present colocalization of FITC-PEG-GOs (green) and F-actin (red). As it can be observed, the samples treated with wortmannin do not show green fluorescence, demonstrating that phagocytosis is the main mechanism for FITC-PEG-GOs uptake.[20] Other mechanisms such as macropinocytosis and clathrin-dependent endocytic pathways can be also involved in the incorporation of FITC-PEG-GOs by hepatic cells, as it can be concluded from the results obtained in the present study by flow cytometry, taking into account the higher sensitivity of this multiparametric technique.

## CONCLUSIONS

To understand the entry mechanisms of PEGylated FITC-GO nanosheets of ca. 100 nm into mammalian cells, the incorporation of this nanomaterial by Saos-2 osteoblasts, HepG2 hepatocytes and RAW-264.7 macrophages was evaluated in the presence of eight inhibitors which specifically affect different endocytosis mechanisms. The results evidence that several processes are involved in FITC-PEG-GOs uptake, depending on the characteristics of each cell type. Although macropinocytosis is the general mechanism of FITC-PEG-GOs internalization observed in the present study, this nanomaterial can also enter through pathways dependent on microtubules in osteoblasts, and through clathrin-dependent mechanisms in hepatocytes and macrophages. Hepatocytes can also phagocytize FITC-PEG-GOs nanosheets. These findings help to understand the interactions at the interface of GO nanosheets and mammalian cells and must be considered in further studies focused on its use for biomedical applications as GO mediated hyperthermia for cancer therapy.

## AUTHOR INFORMATION

### Corresponding Author

*Professor M. T. Portolés. E-mail: portoles@quim.ucm.es.

### Notes

The authors declare no competing financial interest.

## ACKNOWLEDGMENTS

This study was supported by research grants from Comunidad de Madrid (project S2009/MAT-1472) and the Ministerio de Ciencia e Innovación (MICINN) (projects MAT2012-35556 and CSO2010-11384-E Agening Network of Excellence). J. Linares and M. C. Matesanz are greatly indebted to CIBER-BBN and MEC, respectively, for predoctoral fellowships. M. Vila thanks the Spanish Ministry for the RyC grant and the Fundação para a Ciência e Tecnologia (FCT) Investigator Program 2012. We thank FCT, the European Union, QREN, FEDER, COMPETE, for funding the TEMA research unit (PEst-C/EME/UI0481/2013). Gil Gonçalves thanks the FCT for a PostDoc grant (SFRH/BDP/84419/2012). Paula Marques thanks QREN, programme Mais Centro-Programa Operacional Regional do Centro and União Europeia/Fundo Europeu de Desenvolvimento Regional, project Biomaterials for Regenerative Medicine (CENTRO-07-ST24-FEDER-002030) and the FCT Investigator Program 2013. The authors also thank the staff of the Cytometry and Fluorescence Microscopy Center of the Universidad Complutense de Madrid (Spain) for assistance in the flow cytometry and confocal microscopy studies.

## REFERENCES

(1) Novoselov, K. S.; Fal'ko, V. I.; Colombo, L.; Gellert, P. R.; Schwab, M. G.; Kim, K. A Roadmap for Graphene. *Nature* **2012**, *490*, 192−200.

(2) Sun, X.; Liu, Z.; Welsher, K.; Robinson, J. T.; Goodwin, A.; Zaric, S.; Dai, H. Nano-Graphene Oxide for Cellular Imaging and Drug Delivery. *Nano Res.* **2008**, *1*, 203−212.

(3) Zhang, L.; Xia, J.; Zhao, Q.; Liu, L.; Zhang, Z. Functional Graphene Oxide As a Nanocarrier for Controlled Loading and Targeted Delivery of Mixed Anticancer Drugs. *Small* **2010**, *6*, 537−544.

(4) Fan, H.; Wang, L.; Zhao, K.; Li, N.; Shi, Z.; Ge, Z.; Jin, Z. Fabrication, Mechanical Properties, and Biocompatibility of Graphene-Reinforced Chitosan Composites. *Biomacromolecules* **2010**, *11*, 2345−2351.

(5) Depan, D.; Girase, B.; Shah, J. S.; Misra, R. D. Structure-Process-Property Relationship of the Polar Graphene Oxide-Mediated Cellular Response and Stimulated Growth of Osteoblasts on Hybrid Chitosan

Network Structure Nanocomposite Scaffolds. *Acta Biomater.* **2011**, *7*, 3432−3445.
(6) Vila, M.; Matesanz, M. C.; Gonçalves, G.; Feito, M. J.; Linares, J.; Marques, P. A.; Portolés, M. T.; Vallet-Regí, M. Triggering Cell Death by Nanographene Oxide Mediated Hyperthermia. *Nanotechnology* **2014**, *25* (035101), 7.
(7) Yang, K.; Zhang, S.; Zhang, G.; Sun, X.; Lee, S. T.; Liu, Z. Graphene in Mice: Ultrahigh *in Vivo* Tumor Uptake and Efficient Photothermal Therapy. *Nano Lett.* **2010**, *10*, 3318−3323.
(8) Gonçalves, G.; Vila, M.; Portolés, M. T.; Vallet-Regí, M.; Gracio, J.; Marques, P. A. Nano-Graphene Oxide: A Potential Multifunctional Platform for Cancer Therapy. *Adv. Healthcare Mater.* **2013**, *2*, 1072−1090.
(9) Liu, Z.; Robinson, J. T.; Sun, X.; Dai, H. PEGylated Nanographene Oxide for Delivery of Water-Insoluble Cancer Drugs. *J. Am. Chem. Soc.* **2008**, *130*, 10876−10877.
(10) Vila, M.; Portolés, M. T.; Marques, P. A.; Feito, M. J.; Matesanz, M. C.; Ramírez-Santillán, C.; Gonçalves, G.; Cruz, S. M. A.; Nieto-Peña, A.; Vallet-Regí, M. Cell Uptake Survey of Pegylated Nano Graphene Oxide. *Nanotechnology* **2012**, *23*, 465103.
(11) Matesanz, C.; Vila, M.; Feito, M. J.; Linares, J.; Gonçalves, G.; Vallet-Regí, M.; Marques, P. A.; Portolés, M. T. The Effects of Graphene Oxide Nanosheets Localized on F-Actin Filaments on Cell-Cycle Alterations. *Biomaterials* **2013**, *34*, 1562−1569.
(12) Sahay, G.; Alakhova, D. Y.; Kabanov, A. V. Endocytosis of Nanomedicines. *J. Controlled Release* **2010**, *145*, 182−195.
(13) Conner, S. D.; Schmid, S. L. Regulated Portals of Entry into the Cell. *Nature* **2003**, *422*, 37−44.
(14) Mayor, S.; Pagano, R. E. Pathways of Clathrin-Independent Endocytosis. *Nat. Rev. Mol. Cell. Biol.* **2007**, *8*, 603−612.
(15) Mu, Q.; Su, G.; Li, L.; Gilbertson, B. O.; Yu, L. H.; Zhang, Q.; Sun, Y. P.; Yan, B. Size-Dependent Cell Uptake of Protein-Coated Graphene Oxide Nanosheets. *ACS Appl. Mater. Interfaces* **2012**, *4*, 2259−2266.
(16) Zolnik, B. S.; González-Fernández, A.; Sadrieh, N.; Dobrovolskaia, M. A. Nanoparticles and the Immune System. *Endocrinology* **2010**, *151*, 458−465.
(17) Jokerst, J. V.; Lobovkina, T.; Zare, R. N.; Gambhir, S. S. Nanoparticle PEGylation for Imaging and Therapy. *Nanomedicine* **2011**, *6*, 715−728.
(18) Gonçalves, G.; Marques, P. A.; Granadeiro, C.; Nogueira, H. I. S.; Singh, M. K.; Grácio, J. Surface Modification of Graphene Nanosheets with Gold Nanoparticles: The Role of Oxygen Moieties at Graphene Surface on Gold Nucleation and Growth. *Chem. Mater.* **2009**, *21*, 4796−4802.
(19) Chen, J. G.; Hinesley, R.; Kempson, S. A. Dual Action of Colchicine on Hypertonic Activation of System A Amino Acid Transport in Vascular Smooth Muscle Cells. *Life Sci.* **1997**, *61*, 29−37.
(20) Bandmann, V.; Müller, J. D.; Köhler, T.; Homann, U. Uptake of Fluorescent Nano Beads into BY2-cells Involves Clathrin-Dependent and Clathrin-Independent Endocytosis. *FEBS Lett.* **2012**, *586*, 3626−3632.
(21) Bhowmick, T.; Berk, E.; Cui, X.; Muzykantov, V. R.; Muro, S. Effect of Flow on Endothelial Endocytosis of Nanocarriers Targeted to ICAM-1. *J. Controlled Release* **2012**, *157*, 485−492.
(22) Sato, K.; Nagai, J.; Mitsui, N.; Yumoto, R.; Takano, M. Effects of Endocytosis Inhibitors on Internalization of Human IgG by Caco-2 Human Intestinal Epithelial Cells. *Life Sci.* **2009**, *85*, 800−807.
(23) Mäger, I.; Langel, K.; Lehto, T.; Eiríksdóttir, E.; Langel, Ü. The Role of Endocytosis on the Uptake Kinetics of Luciferin-Conjugated Cell-Penetrating Peptides. *Biochim. Biophys. Acta* **2012**, *1818*, 502−511.
(24) Schulz, W. L.; Haj, A. K.; Schiff, L. A. Reovirus Uses Multiple Endocytic Pathways for Cell Entry. *J. Virol.* **2012**, *86*, 12665−12675.
(25) Yang, C. Y.; Tai, M. F.; Lin, C. P.; Lu, C. P.; Lu, C. W.; Wang, J. L.; Hsiao, J. K.; Liu, H. M. Mechanism of Cellular Uptake and Impact of Ferucarbotran on Macrophage Physiology. *PLoS One* **2011**, *6*, 7.
(26) Kiyoshima, D.; Kawakami, K.; Hayakawa, K.; Tatsumi, H.; Sokabe, M. Force- and $Ca^{2+}$-Dependent Internalization of Integrins in Cultured Endothelial Cells. *J. Cell. Sci.* **2011**, *124*, 3859−3870.
(27) Liu, X.; Huang, N.; Li, H.; Jin, Q.; Ji, J. Surface and Size Effects on Cell Interaction of Gold Nanoparticles with Both Phagocytic and Nonphagocytic Cells. *Langmuir* **2013**, *29*, 9138−9148.
(28) Yue, H.; Wei, W.; Yue, Z.; Wang, B.; Luo, N.; Gao, Y.; Ma, D.; Ma, G.; Su, Z. The Role of the Lateral Dimension of Graphene Oxide in the Regulation of Cellular Responses. *Biomaterials* **2012**, *33*, 4013−4021.
(29) Jones, A. T. Macropinocytosis: Searching for an Endocytic Identity and Role in the Uptake of Cell Penetrating Peptides. *J. Cell. Mol. Med.* **2007**, *11*, 670−684.
(30) Kruth, H. S.; Jones, N. L.; Huang, W.; Zhao, B.; Ishii, I.; Chang, J.; Combs, C. A.; Malide, D.; Zhang, W. Y. Macropinocytosis Is the Endocytic Pathway that Mediates Macrophage Foam Cell Formation with Native Low Density Lipoprotein. *J. Biol. Chem.* **2004**, *280*, 2352−2360.
(31) Koivusalo, M.; Welch, C.; Hayashi, H.; Scott, C. C.; Kim, M.; Alexander, T.; Touret, N.; Hahn, K. M.; Grinstein, S. Amiloride Inhibits Macropinocytosis by Lowering Submembranous pH and Preventing Rac1 and Cdc42 Signaling. *J. Biol. Chem.* **2010**, *188*, 547−563.
(32) Cantley, L. C. The Phosphoinositide 3-Kinase Pathway. *Science* **2002**, *6*, 1655−1657.
(33) Soji, T.; Murata, Y.; Ohira, A.; Nishizono, H.; Tanaka, M.; Herbert, D. C. Evidence that Hepatocytes can Phagocytize Exogenous Substances. *Anat. Rec.* **1992**, *233*, 543−546.
(34) Tuma, P. L.; Finnegan, C. M.; Yi, J. H.; Hubbard, A. L. Evidence for Apical Endocytosis in Polarized Hepatic Cells: Phosphoinositide 3-Kinase Inhibitors Lead to the Lysosomal Accumulation of Resident Apical Plasma Membrane Proteins. *J. Cell. Biol.* **1999**, *145*, 1089−1102.
(35) Fujimoto, T.; Kogo, H.; Nomura, R.; Une, T. Isoforms of Caveolin-1 and Caveolar Structure. *J. Cell. Sci.* **2000**, *113*, 3509−3517.
(36) Hou, C. H.; Tang, C. H.; Hsu, C. J.; Hou, S. M.; Liu, J. F. CCN4 Induces IL-6 Production through $\alpha\phi\beta$5 Receptor, PI3K, Akt, and NF-$\kappa$B Signaling Pathway in Human Synovial Fibroblasts. *Arthritis Res. Ther.* **2013**, *15*, R19.